Tracking sustained chaos: A segmentation method

Ioana Triandaf and Ira B. Schwartz*
Special Project for Nonlinear Science, Code 6700.3, Plasma Physics Division, U.S. Naval Research Laboratory, Washington, DC 20375-5346
(Received 4 June 1999; revised manuscript received 5 June 2000)

We introduce a segmentation control method to sustain chaotic transients in dynamical systems. The sustained transient can be tracked as a system parameter is substantially varied, allowing sustained chaotic transients far away from crisis parameter values. The method is applied to a chaotic CO_2 laser as well as to a hyperchaotic continuum mechanics model. [S1063-651X(00)12009-4]

PACS number(s): 05.45.Jn, 05.45.Gg, 46.40.Ff, 42.65.Sf

INTRODUCTION

Chaos can be a desirable feature in many applications. In biology, the disappearance of chaos may signal pathological phenomena [1–3]. In mechanics, chaos could be induced to spread modal energy at resonance in continua [4,5], and may also be induced to achieve optimal machine tool cutting in materials [6]. Chaos is also important in nonlinear optical communication schemes [7]. In general, however, chaotic attractors may persist over small parameter regions, whereas chaotic transients persist over large regions in the form of chaotic saddles which result from a crisis [8]. Therefore, it is fundamental to extend the concept of controlling unstable dynamical objects to that of chaotic transients, which we call sustained chaos.

Sustained chaos was introduced in one-dimensional maps in [2,9], and control of chaotic saddles for two-dimensional (2D) maps was presented in [10]. Sustained chaos in the presence of other nonchaotic attractors was also achieved [11] by using the natural dynamics of unstable states lying on the basin boundary separating a periodic attractor from chaotic transients, called basin boundary saddles. Basin saddle methods were subsequently tested experimentally on a low-dimensional system [9]. If one applies this method to high-dimensional systems possessing complicated behavior, identification of the relevant basin boundary saddles may be quite difficult. Therefore, a different approach is required.

The proposed method consists in targeting points near a chaotic transient, once the iterates reach a neighborhood of an undesired attractor. Targeting is done so that the natural dynamics of the system will engage again the iterations in chaotic motion. By making a brief parameter fluctuation, the attractor is forced to be a repeller so that a point which lies on the previously existing chaotic transient can be targeted. So instead of landing on the attractor, the iterations will reach a region of phase space where a chaotic transient is present, causing the chaotic motion to be reexcited. Targeting is done close to the attractor, monitoring a chosen neighborhood, and modeling the system around the attractor based on a local linear approximation which can be obtained from a model as well as from real data. The method takes into account both the topology of the phase space about the attractor and the escape regions (see Fig. 1 and Fig. 2 below). The main improvement over previously existing methods for sustaining chaos is that the sustained chaotic transient can be tracked as a parameter is varied. Due to smoothly changing characteristics of the chosen regions and related topology, the sustained chaotic transient may be recreated at parameter values well beyond the original crisis value. (See [12–14] for the general theory of tracking unstable orbits.)

We begin by stating our assumptions from a topological viewpoint. The relevant topology is shown in Fig. 1 for a general map f, where A denotes the attractor and CT the chaotic transient region. In this schematic we show the attractor, A, the basin saddle which provoked the disappearance of the attractor and the stable and unstable manifolds of this basin saddle. We assume that the attractor A is proximate to the stable manifold of the saddle which forms the basin boundary of the attractor. In Fig. 1 we circle a neighborhood of the attractor A which intersects both the basin of attraction of A and a region containing points which approach the chaotic transient. This is the neighborhood monitored in this algorithm and control is activated every time iterations enter such a neighborhood. Let $f^{-1}(B)$ be a point on the stable

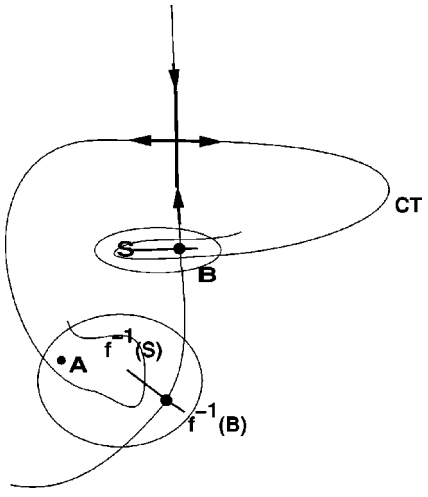

FIG. 1. Global topology setup for sustained chaos based on a basin boundary saddle. The map, f, maps the plane into itself. Point A denotes the attractor. B and its preimage, $f^{-1}(B)$, lie on the stable manifold of the basin boundary saddle. S denotes a line segment through B, and $f^{-1}(S)$ is its preimage. CT denotes the region containing the chaotic transient.

*Present address: Center for Biomolecular Science and Engineering, Code 6900.IS, Naval Research Laboratory, W. Washington, DC 20375.

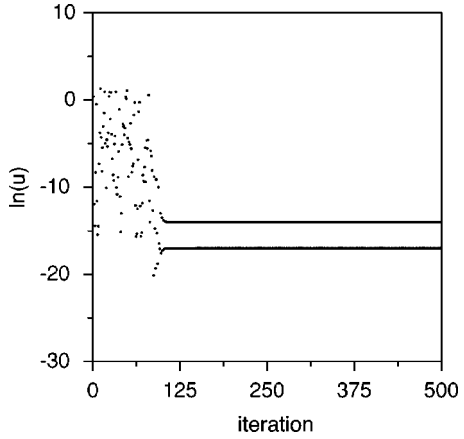

FIG. 2. Iterations for $\ln(u)$ at $\delta=1.88$ illustrating a chaotic transient landing on a period-4 attractor. Every other iterate is shown.

manifold of the drawn saddle. Consider a segment $f^{-1}(S)$ passing through $f^{-1}(B)$. The map takes the segment $f^{-1}(S)$ and the point $f^{-1}(B)$ into segment S and point B, respectively. Segment S and point B both lie in a neighborhood of the basin saddle. Therefore, parameter perturbations in the preimage neighborhood, near the attractor, will be represented similarly in the original image near the saddle due to continuity. Notice the segment $f^{-1}(S)$ crosses the stable manifold, and intersects the basin of attraction of A and the chaotic transient. The end points of $f^{-1}(S)$ will separate dynamically: one end point, E_A, moving towards the attractor and the other, E_{CT} starting to move chaotically.

In the actual implementation of this algorithm, say in an experiment, we need to probe for the relevant topology. This is done by finding a segment such as $f^{-1}(S)$ with end points such that one goes to the attractor and the other one goes to the chaotic region. Since the two diverging points create a segment which straddles the stable manifold, the procedure is called segmentation. The process of segmentation guarantees that we are close to the boundary of the attractor, and the end point which is mapped into the chaotic transient region represents a good candidate for targeting. A parameter fluctuation which sends the iterates to such a point has the result that subsequent iterates will be chaotic since they are attracted to the chaotic transient. Chaos is reactivated by repeating the monitoring and actuation process based on segmentation [15].

We note that since the segmentation procedure straddles a stable manifold, it is similar in spirit to the proper interior maximum (PIM) triple procedure introduced in [16] for computing orbits which lie on one-dimensional manifolds.

SUSTAINING AND TRACKING CHAOTIC TRANSIENTS

To sketch the main ideas for sustaining and tracking chaos, we consider a generic high-dimensional Poincare map T:

$$\mathbf{x}_{n+1}=T(\mathbf{x}_n,\delta_n), \tag{1}$$

where $\delta_n=\delta_0+\Delta\delta_n$ is the parameter we adjust to sustain chaos. Assume T has a chaotic transient, and an attractor denoted by fixed point $(\mathbf{x}_0,\delta_0)$ at parameter δ_0. Applying the algorithm to Eq. (1) proceeds as follows: every time the iterations reach a prescribed neighborhood of the attractor $\mathbf{x}_0$, control is activated. The parameter perturbation is chosen to target a preassigned value in a neighborhood of the end point, E_{CT}, $N(E_{\mathrm{CT}})$, contained in a previously existing chaotic transient. So the value of $\mathbf{x}_{n+1}$ is preassigned.

Targeting is accomplished by using two steps. First, pole placement [17], which has been previously applied to the control of chaos using time series embedding, is used to destabilize the attractor [18]. Then the destabilized system is used to target a point in $N(E_{\mathrm{CT}})$. Linearizing T about the periodic attracting point $(\mathbf{x}_0,\delta_0)$, we obtain

$$\mathbf{x}_{n+1}-\mathbf{x}_0=\mathbf{A}(\mathbf{x}_n-\mathbf{x}_0)+\mathbf{B}(\delta_n-\delta_0), \tag{2}$$

where $\mathbf{A}$ is the derivative of the map with respect to $\mathbf{x}$, and $\mathbf{B}$ is the derivative of the map with respect to δ at $(\mathbf{x}_0,\delta_0)$. The perturbation of the parameter is given by

$$\delta_n-\delta_0=-\mathbf{K}(\mathbf{x}-\mathbf{x}_0). \tag{3}$$

The vector K from Eq. (3) is chosen in such a way that the target point $\mathbf{x}_{n+1}$ will lie inside $N(E_{\mathrm{CT}})$. This changes briefly the attractor into a saddle or into a repeller while targeting simultaneously. Since the attractors have well defined transients in a local neighborhood, it is easy to acquire linear least-squares approximations to Eq. (2) from embedded time series [18] in order to derive the matrix $\mathbf{A}$ and the vector $\mathbf{B}$ from experimental data. Tracking is done by updating the linearized model (2) as δ_0 is changed, which we now describe.

The present algorithm allows for continuing, or tracking, the sustained chaotic state as the parameter is increased without any premeasuring of the system. Increasing δ_0 by a small amount, say h, we want chaos to persist at the new parameter value. As the parameter is increased, the position of the attractor changes continuously along with the relevant saddle. This saddle is connected to the stable manifold which is contained in the neighborhood which we target (see Fig. 1). However, the previous target point may not be suitable as a target point since it may no longer lie across the stable manifold. That is, the line segment connecting two diverging points at parameter δ_0 may no longer satisfy the hypotheses in Fig. 1 at the new parameter value, δ_0+h. Therefore, the position of the attractor has to be updated as well as the target point. Once these new values are determined, the hypotheses of the topology in Fig. 1 will be satisfied, and the segmentation procedure can be implemented as before.

The new position of the attractor and its neighborhood can be easily found since the dynamics will asymptotically approach this attractor naturally. Next we need to have an approximate location of the boundary separating the attractor and the chaotic transient at the new parameter value. We determine the approximate boundary by locating a point which diverges from the attractor neighborhood. Some trial and error has to be used for this step in a real experiment. Given a model, a rigorous approach would be to locate the basin boundary accurately using an appropriate algorithm such as the PIM triple procedure [16]. In practice, probing a few target points is sufficient to approximate a segment which crosses the boundary defined by a stable manifold.

To make this probing effective, we proceed as follows. We start by using the previous target point as our new target

point. If the previous target point is attracted to the new attractor, then we turn the attractor at the new parameter value into a repeller using pole-placement methods [18]. Now that local neighborhood about the attractor is repelling, we can pick a few points distributed around it and see where the dynamics sends them in the short time. If one of these points evolves into chaotic motion, we choose that point as our target point and use it to sustain chaos at this new parameter value. We define that point to be targetable if the point is parametrically accessible from the repelling neighborhood. That is, if points begin to approach the attractor, creating a repeller enables the location of a targetable point. Once a targetable point is located, a segment may be constructed between an attracting point and the targetable point which intersects the stable manifold.

In contrast to acquiring a targetable point, now suppose all of the chosen points fall back on the attractor. The indication is that the attractor is too far from the boundary and tracking cannot proceed any further under the hypotheses illustrated in Fig. 1. This is due to the fact that a segment intersecting the boundary cannot be constructed for the sample of points considered.

At parameter values near the crisis value, the problem of finding a segment intersecting the boundary does not exist when the crisis is near a saddle-node bifurcation point. The attractor is initially close to its basin boundary by the nature of the type of crisis we consider, so tracking can be done as we increase the parameter such that we are close to the crisis value. How far we may extend the segmentation procedure for larger values of δ depends on the problem being considered. In the case of the low-dimensional model considered below, we were able to pursue the tracking procedure considerably past the crisis parameter value. Therefore, the success of tracking depends on the attractor neighborhood remaining sufficiently close to the stable manifold boundary, which is always the case initially at the crisis value, so delay of the crisis is always possible.

APPLICATIONS OF TRACKING AND SUSTAINING CHAOS

A low-dimensional model

We use a periodically forced laser to test our ideas since the topology of the manifolds which form chaotic transients arising from horseshoe dynamics is well known [19]:

$$\frac{du}{dt} = -u[\,\delta\cos(\Omega t+\psi)-z\,],$$
$$\frac{dz}{dt} = -\epsilon_1 z - u - \epsilon_2 z u + 1, \tag{4}$$

where u and z denote (scaled) intensity and population inversion. δ represents the amplitude of the drive. The fixed parameters and their values are $\epsilon_1 = 0.09$, $\epsilon_2 = 0.003$, and $\psi = 0$. The original model was introduced in [20], and control and tracking of unstable periodic orbits are done in [11,13]. Other papers which have analyzed this model in various applications appear in [21] and [22].

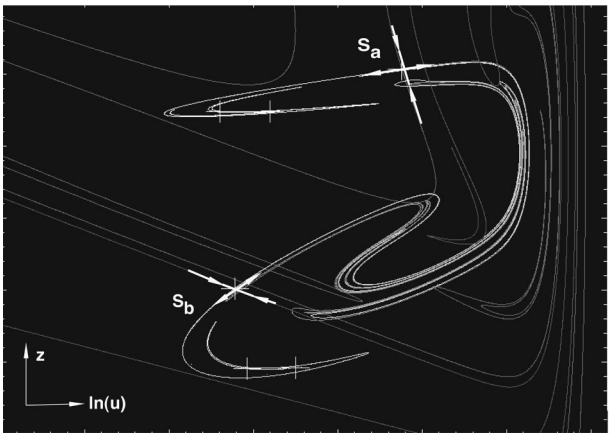

FIG. 3. The topology setup for the laser model in Eq. (4) when $\delta = 1.88$. S_a and S_b denote period-2 basin boundary saddles. The crosses denotes the period-4 attractor.

For δ slightly past a critical value δ_c, a chaotic saddle is created due to the unstable manifold of the basin boundary saddle crossing its stable manifold. Almost all points in the region near the saddle now converge to a period-4 attractor which has period-doubled off the period-2 branch. A chaotic transient typically settles into a period-4 attractor after about 100 iterations as shown in Fig. 2.

In Fig. 3 we show the topology of the phase space corresponding to Eq. (4). We notice in this figure the attractor of period 4 and the period-2 basin saddle with its stable and unstable manifolds. In this figure, a horseshoe is created from the right; i.e., the unstable manifold to the right of the stable manifold crosses the stable manifold near S_a. Almost all points in the region near the saddle now converge to a period-4 orbit which has period-doubled off the period-2 branch. The purpose of our method is to make the chaotic transients persist by preventing the flow from being captured by the attracting orbit.

In Fig. 4 we show the iterates of T (dots) after applying the sustained chaos algorithm guided by Eq. (3). The chaotic

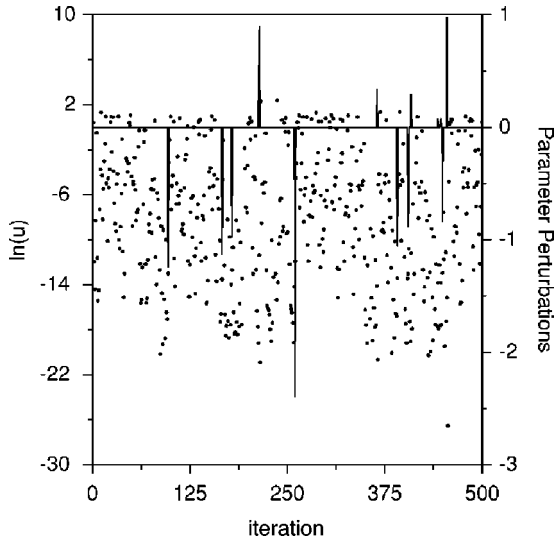

FIG. 4. Sustained chaos (dots) using parameter perturbations (lines), $\delta_n - \delta_0$, where $\delta_0 = 1.88$. The map T is a period-2 map, and the attractor (not shown) is of period 4.

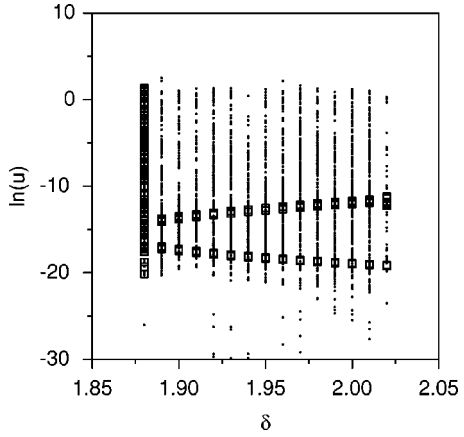

FIG. 5. Sustained chaos (dots) is tracked as the parameter δ is increased discretely. The absorbing attractors (open squares) are also shown as a bifurcation diagram.

transients were prolonged on average by 350 period-2 iterations, which translates to 700 iterations of the drive period. In Fig. 4, the right axis illustrates the parameter perturbations used to sustain the chaotic saddle. Notice that only 13 parameter fluctuations were needed. To justify that indeed the fluctuations resulted in induced chaotic behavior, we found that the maximum Lyapunov exponent calculated from the linear variational equations along the parametrically perturbed trajectory in Fig. 4 was approximately 0.14.

In the above numerical experiments we applied the segmentation-tracking technique every other period, activating parameter perturbations every time the dynamics lands within a neighborhood of a (period-4) attractor. The vector K was reconstructed at each increment in δ. At each parameter value we sustained 400 chaotic iterates (dots) which appear along vertical lines in Fig. 5. Also plotted is the bifurcation picture of attractors without parameter control (open boxes). We notice from Fig. 5 that the range over which tracking is possible removes the restriction of sustaining chaos close to a crisis parameter value.

Periodic saddles which are responsible for the observed global dynamical behavior typically persist over very large ranges of parameter values, which is the case for Eq. (1) [19]. Tracking sustained chaos is possible since these saddles naturally persist, so the global structure of the stable and unstable manifolds of this persisting periodic saddle intersect transversally as they did for the original chaotic transient. As we perturb the system, the horseshoe dynamics is being reexcited and chaos is induced, as evidenced by the positive Lyapunov exponent.

A high-dimensional model

We apply the above procedure to a high-dimensional coupled-pendulum model. In [5], new dynamical behavior was presented for a system consisting in a forced damped pendulum attached to a stiff rod which is flexible and moves periodically in a vertical plane. The system was examined when operating in a resonant mode, where the pendulum frequency is half that of the fundamental frequency of the rod. It is known that when the rod is sufficiently stiff, the dynamics resides on a global slow invariant manifold, the rod being slaved to the motion of the pendulum [4], so the dynamics is a perturbation of a parametrically driven pendulum. When operating at resonance, there exists a critical amplitude of the driving force that causes an abrupt change from periodic behavior to high-dimensional hyperchaotic behavior where there are two or more positive Lyapunov exponents. Chaos appears discontinuously, without a bifurcation sequence to chaotic behavior. Chaos appears as a subcritical bifurcation point since it exhibits hysteretic behavior as a function of the amplitude of the forcing.

We apply the tracking sustained chaos algorithm for the high-dimensional continuum mechanics model for the set of parameter values which exhibits hyperchaos (more than one positive Lyapunov exponent). This model describing a pendulum attached to a flexible support is derived in [4]. The support of the pendulum is a linear viscoelastic rod restricted to undergo planar vertical motion subject to a time-dependent motion $x_A(t)=\alpha\cos\omega t$, at its upper end, A. $X_B(\tau)$ is the motion of the bottom of the rod relative to the support. The rod equation (dimensionless) modeling the displacement field, V, and angular displacement of the pendulum θ is given by

$$\ddot{\theta}=-[1-\ddot{V}(\xi=1,\tau)+\ddot{X}_A(\tau)]\sin(\theta)-2\zeta_p\dot{\theta}, \tag{5}$$

$$\frac{\mu^2\pi^2}{4}V_{,\tau\tau}(\xi,\tau)=V_{,\xi\xi}(\xi,\tau)+2\zeta_r\mu V_{,\tau\xi\xi}(\xi,\tau)-\frac{\mu^2\pi^2}{4}\ddot{X}_A(\tau), \tag{6}$$

$$V(\xi=0,\tau)=0,$$

$$V_{,\xi}(\xi=1,\tau)=-\frac{\mu^2\beta\pi^2}{4}[1-T\cos(\theta)], \tag{7}$$

where

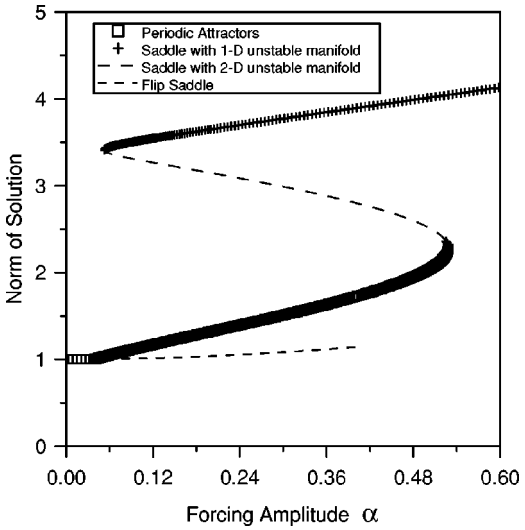

FIG. 6. A bifurcation diagram showing the branches of periodic solutions as a function of α for the one-mode model. Notice that there is saddle-saddle bifurcation opening to the right. The lower branch of saddles has a two-dimensional unstable manifold. See text for details and parameter values.

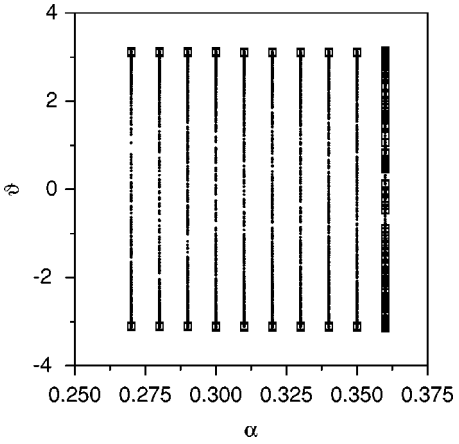

FIG. 7. Sustained chaos (dots) for the coupled rod pendulum is tracked as the parameter α is decreased. The absorbing periodic attractors (open squares) are shown as a bifurcation diagram.

$$T=\dot{\theta}^2+[1-\ddot{X}_B(\tau)]\cos(\theta). \tag{8}$$

The variable $V(\xi,\tau)$ denotes the normalized displacement field with respect to the normalized static displacement field. Equation (7) gives the boundary conditions for the coupled rod (6). Equation (8) gives the normalized tension T along the pendulum arm. In [5], a bifurcation to high-dimensional hyperchaos was shown for the above PDE-ODE system, where both the number of active modes and the number of positive Lyapunov exponents increase discontinuously, making the system high dimensional and hyperchaotic.

The solution of Eq. (5) is expanded using a Galerkin approximation in space and a set of coupled oscillators is obtained. In what follows, a first-order truncation yields a linear-nonlinear driven coupled oscillator system. Fixed parameter values are $\mu=0.577$, $\xi_p=\xi_r=0.01$, $\omega=1.952$, $\beta=1$. (See [5] for details.) The discrete dynamics generated by sampling at the forcing frequency is four-dimensional, and we have found that the chaotic transient (when sustained) has two positive Lyapunov exponents, with values 0.21 and 0.04 when $\alpha=0.36$. The perturbation parameter we use for tracking sustained chaos is α.

The bifurcation structure of the one-mode model derived from Eqs. (5)–(8) is shown in Fig. 6 as a function of forcing amplitude α. In Fig. 6, there are two coexisting branches of saddles in the parameter region of interest, in addition to a coexisting attracting branch. One branch of saddles has a one-dimensional unstable manifold, while the other has a two-dimensional unstable manifold. (Details will appear elsewhere.) The high-dimensional unstable direction is conjectured to be the source of hyperchaotic transients; i.e., chaos having more than one positive Lyapunov exponent. This situation shown in Fig. 6 is more complicated than the one presented in [23] since (i) chaos is hyperchaotic with two positive Lyapunov exponents, (ii) a connecting branch of saddles has a two-dimensional unstable manifold, and (iii) it is not clear which saddle is the basin boundary saddle. Such complications make it difficult to sustain chaos based on basin boundary saddle methods such as those in [11] and [23]. However, the segmentation-tracking procedure allows one to overcome such difficulties.

In Fig. 7 we show the tracked chaotic state for 10 steps, started at $\alpha=0.36$, and then tracked for decreased α. For each parameter value, the chaotic iterations (dots) appear in Fig. 7 along a vertical line. The same trajectory, when the algorithm is not applied, would collapse on the periodic attractor (shown as open squares). The parameter perturbations used to obtain Fig. 7 are shown in Fig. 8 for the entire run as a function of iteration. For each fixed parameter in Fig. 7, 500 iterations were computed.

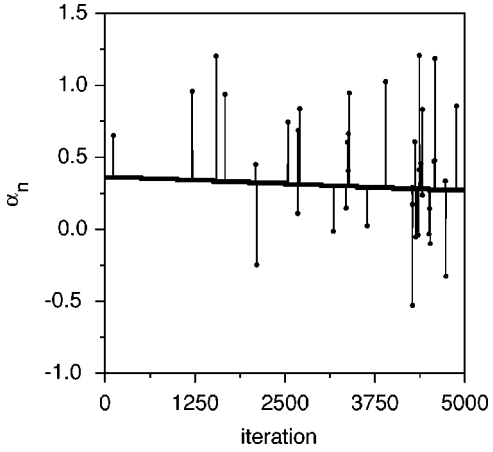

FIG. 8. Parameter values and perturbations of α used to track sustained chaos in the rod-pendulum model.

CONCLUSION AND DISCUSSION

Tracking sustained chaos is an improvement over previous methods where chaos was sustained only at a fixed parameter value [2,11]. Such a method requires only partial knowledge of the phase space and applies to systems modeled from time series, which makes it suitable for experiments. A definitive advantage is that the technique can be more easily implemented than previous methods when applied to higher dimensional systems since the accurate description of stable and unstable manifolds governing the crisis may be extremely hard to compute in higher dimensions.

Other approaches to sustained chaos can be found in [2,9,24], where the algorithm requires accurate knowledge of escape regions in phase space where chaos disappears, as well as knowledge of the preiterations of this region. An analytic scheme for sustained chaos was introduced in [25] that uses state variable control, but modifies explicitly the governing dynamical model.

Instead of preventing escape to an attractor in advance as done in [2] and [9], our approach is to take a global view of the phase space, inhibit the absorbing attractor, and target a chosen neighborhood. This amounts to briefly changing the nature of the attractor by adjusting temporarily an accessible system parameter. The method succeeds whenever a suitable topology of phase space is present, namely the attractor which absorbs the chaotic transient is close to the basin boundary between the attractor and the transient. In this way, points across the basin boundary are accessible by targeting. As a result of targeting, the natural dynamics of the system is used to recreate chaos.

ACKNOWLEDGMENT

This research was supported by the Office of Naval Research.

[1] A. L. Goldberger, *Getting to the Heart of Chaos: Nonlinear Dynamics in Clinical Cardiology*, in *Proceedings of the 1st Experimental Chaos Conference*, edited by Sandeep Vohra *et al.* (World Scientific, Singapore, 1991).
[2] W. Yang, M. Ding, A. J. Mandell, and E. Ott, Phys. Rev. E **51**, 102 (1995).
[3] S. J. Schiff, K. Jerger, D. H. Duong, T. Chang, M. L. Spano, and W. L. Ditto, Nature (London) **370**, 615 (1994).
[4] I. T. Georgiou and I. B. Schwartz, SIAM (Soc. Ind. Appl. Math.) J. Appl. Math. **59**, 1178 (1999).
[5] I. B. Schwartz and I. T. Georgiou, Phys. Lett. A **242**, 307 (1998).
[6] H. Abarbanel, *Analysis of Observed Chaotic Data* (Springer, New York, 1996), pp. 1–9; Francis Moon (private communication).
[7] G. D. VanWiggeren and R. Roy, Science **279**, 1198 (1998).
[8] G. Grebogi, E. Ott, and J. A. Yorke, Physica D **7**, 181 (1983).
[9] V. In, S. E. Mahan, W. L. Ditto, and M. Spano, Phys. Rev. Lett. **74**, 4420 (1995).
[10] Y. C. Lai and C. Grebogi, Phys. Rev. E **49**, 1094 (1994).
[11] I. B. Schwartz and I. Triandaf, Phys. Rev. Lett. **77**, 4740 (1996).
[12] I. B. Schwartz and I. Triandaf, Phys. Rev. A **46**, 7439 (1992).
[13] I. B. Schwartz and I. Triandaf, *Control and Prediction in Seasonally Driven Epidemic Models*, in *Predictability and Nonlinear Modeling in Natural Sciences and Economics*, edited by J. Grasman and G. van Straten (Kluwer, Dordrecht, 1994), pp. 216–228.
[14] I. B. Schwartz, T. W. Carr, and I. Triandaf, Chaos **7**, 664 (1997).
[15] If the attractor is far from this basin boundary, a different technique has to be used, such as goal dynamics, to lead the dynamics from a point near the attractor to a point across its basin boundary. This will be the subject of a future paper.
[16] H. E. Nusse and J. A. Yorke, Ergod. Th. Dynam. Sys. **11**, 189 (1991).
[17] K. Ogata, *Modern Control Engineering* (Prentice-Hall, Englewood Cliffs, NJ, 1990).
[18] F. Romeiras, C. Grebogi, E. Ott, and W. P. Dayawansa, Physica D **58**, 165 (1992).
[19] I. B. Schwartz, Phys. Rev. Lett. **60**, 1359 (1988).
[20] F. T. Arecchi *et al.*, Phys. Rev. Lett. **49**, 1217 (1982).
[21] D. Dangoisse, P. Glorieux, and D. Hennequin, Phys. Rev. Lett. **57**, 2657 (1986).
[22] Ira B. Schwartz and T. E. Erneux, SIAM (Soc. Ind. Appl. Math.) J. Appl. Math. **54**, 1083 (1994).
[23] V. In, M. Spano, and M. Ding, Phys. Rev. Lett. **80**, 700 (1998).
[24] K. Kacperski and J. A. Holyst, Phys. Rev. E **55**, 5044 (1997).
[25] G. Chen (unpublished).